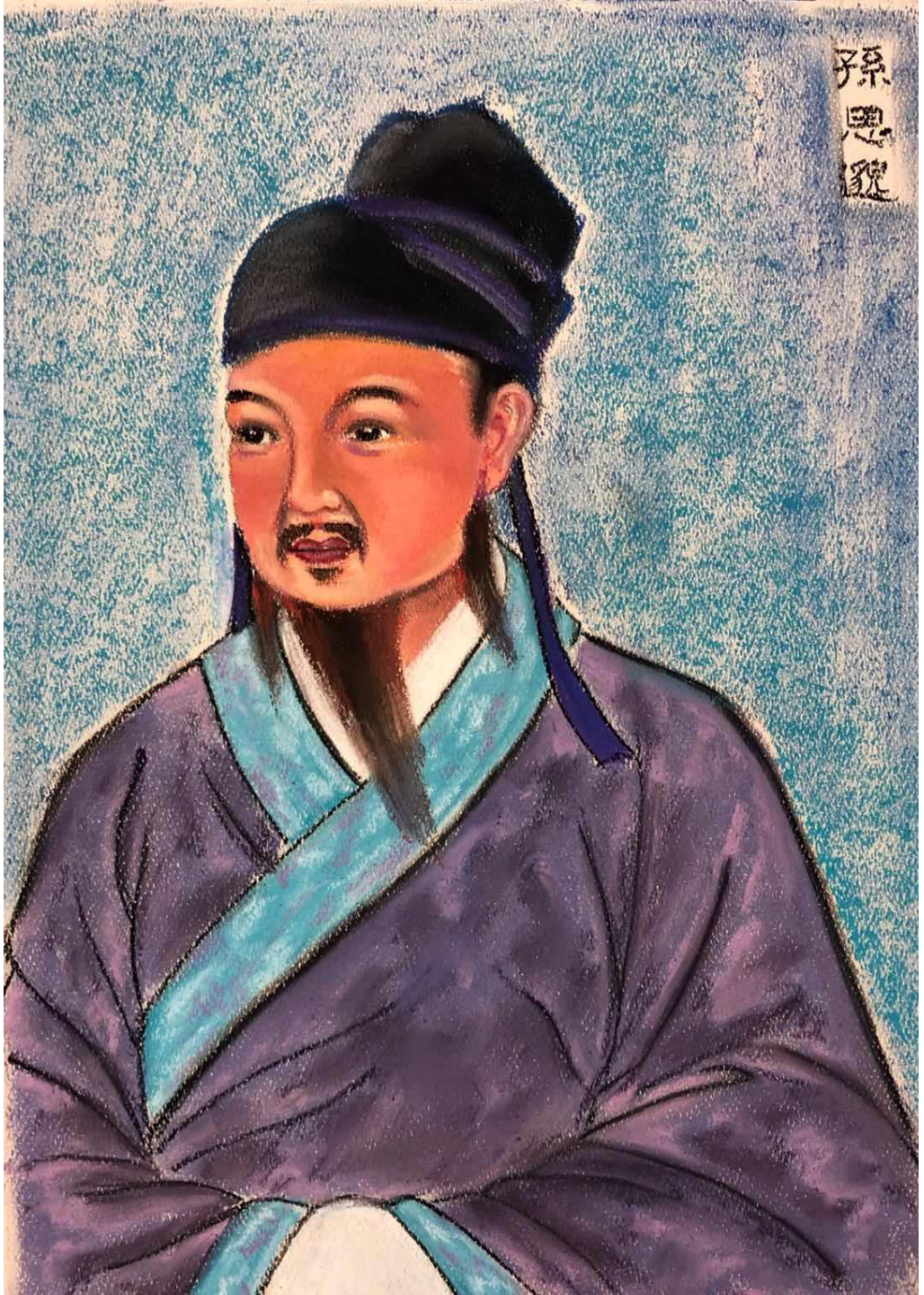
孫思邈

Figure 1. Artistic depiction of San Si Miao (original drawings from historical representations by Xin Zhang). Miao described the use of deer and sheep thyroid to treat patients with goiter. This represented the early description of organ
He was called at that time the “King of Medicine”

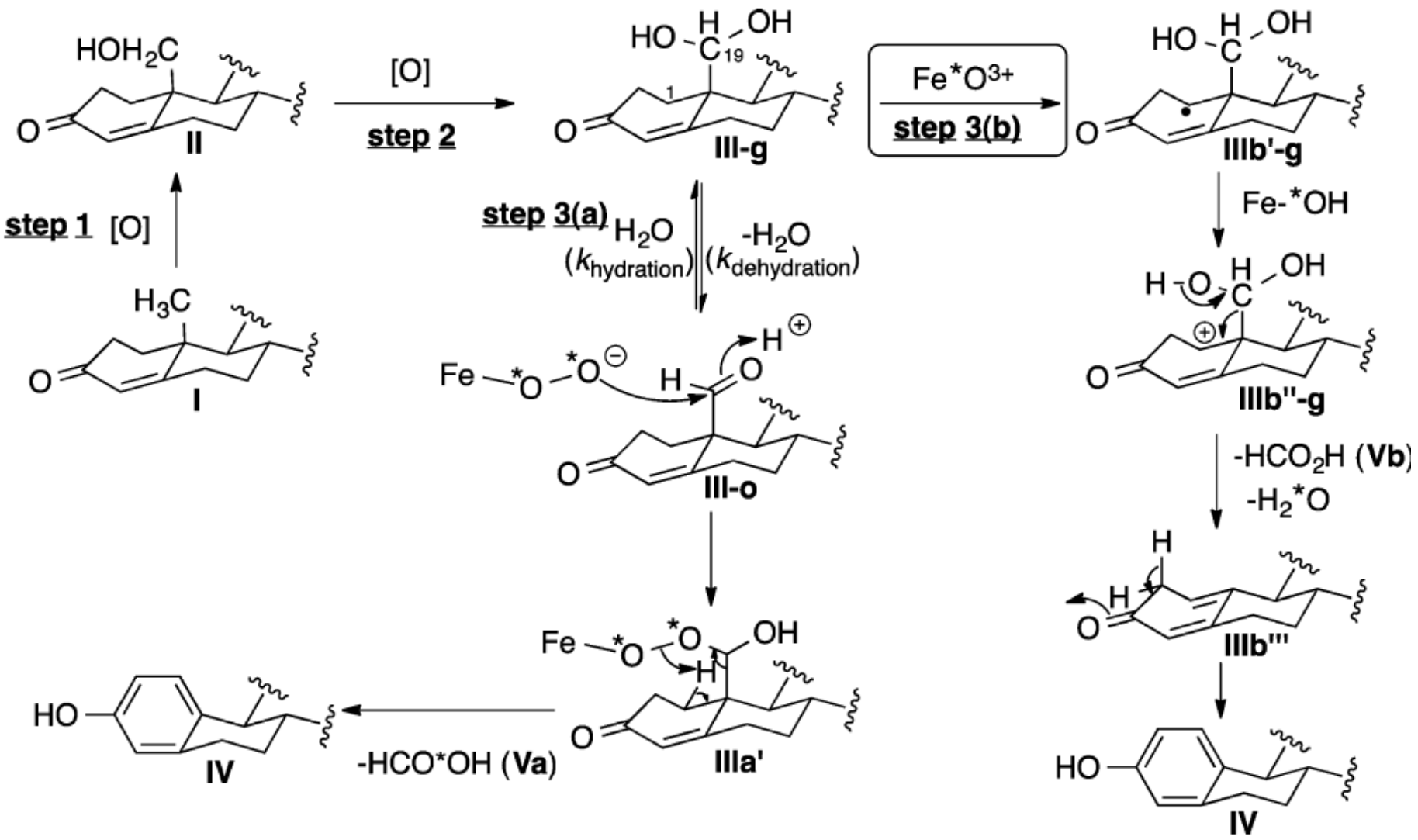
HOH2C
II
[O]
step 2
HO
H
OH
C19
1
III-g
Fe*O3+
step 3(b)
IIIb'-g
Fe-*OH
step 1 [O]
H3C
I
step 3(a)
H2O
(khydration)
-H2O
(kdehydration)
IIIb''-g
-HCO2H (Vb)
-H2*O
III-o
IIIb'''
Fe
*O
H
OH
IIIa'
HO
IV
-HCO*OH (Va)
HO
IV

Figure 2. Reaction mechanism of aromatase P450 with the individual steps involved. The reaction begins with abstraction of the 1β-hydrogen atom by FeO^{3+} Further electron transfer yields the C-1 carbocation and proton abstraction from the *gem*-diol by Fe-OH and rearrangement yields formic acid and subsequently estrogen . Alternatively, oxygen rebound can occur to the A ring to yield the hydroxyl 19-aldehyde seen by LC-MS. In an alternative initial reaction, FeO^{3+} abstracts the C-19 hydrogen atom. Oxygen rebound yields a *gem*-triol, which degrades to the 19-carboxylic acid. Reproduced from Yoshimoto and Guengerich (1) with permission of the publishers for online and print versions.

Structure of the human aromatase (*CYP19*) gene showing tissue-specific promoter usage

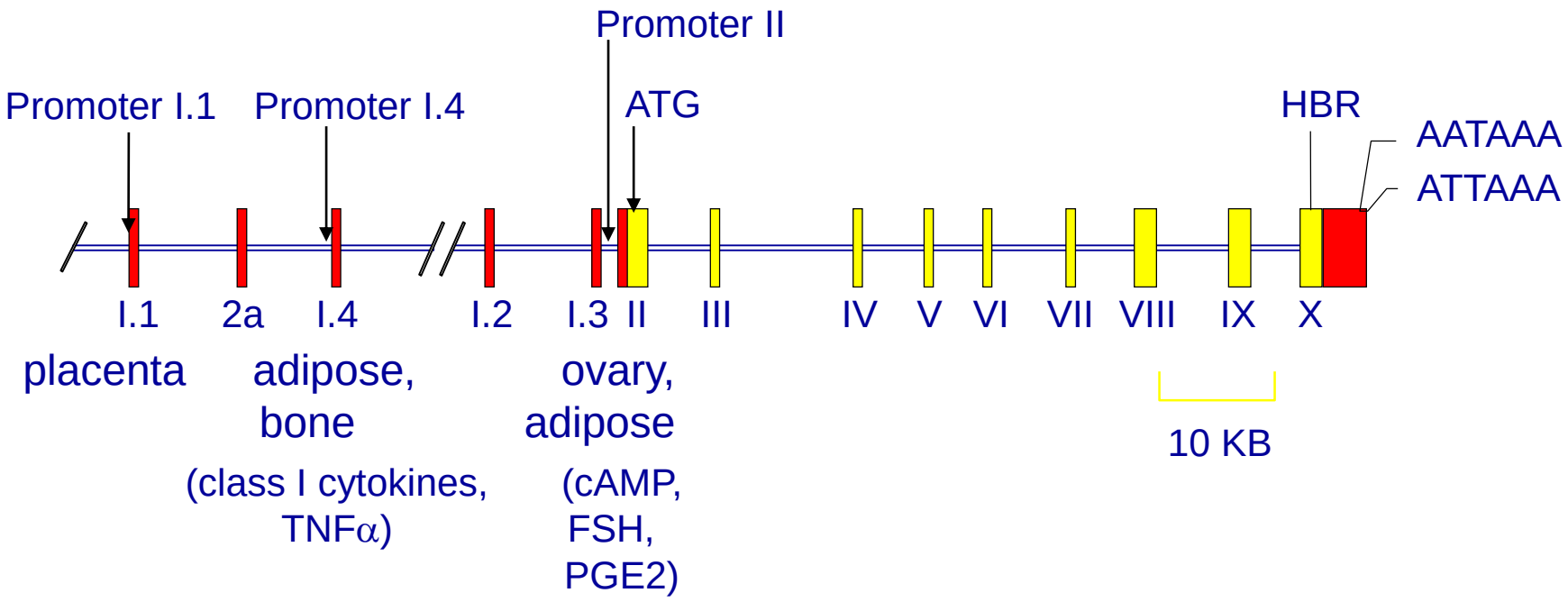

Figure 3. Structure of the human aromatase (CYP19) gene and its alternate promoters. Note in the footnote in the text that the nomenclature of the alternative promotors differs in the literature (2). Reproduced with the permission of the publishers for online and print versions.

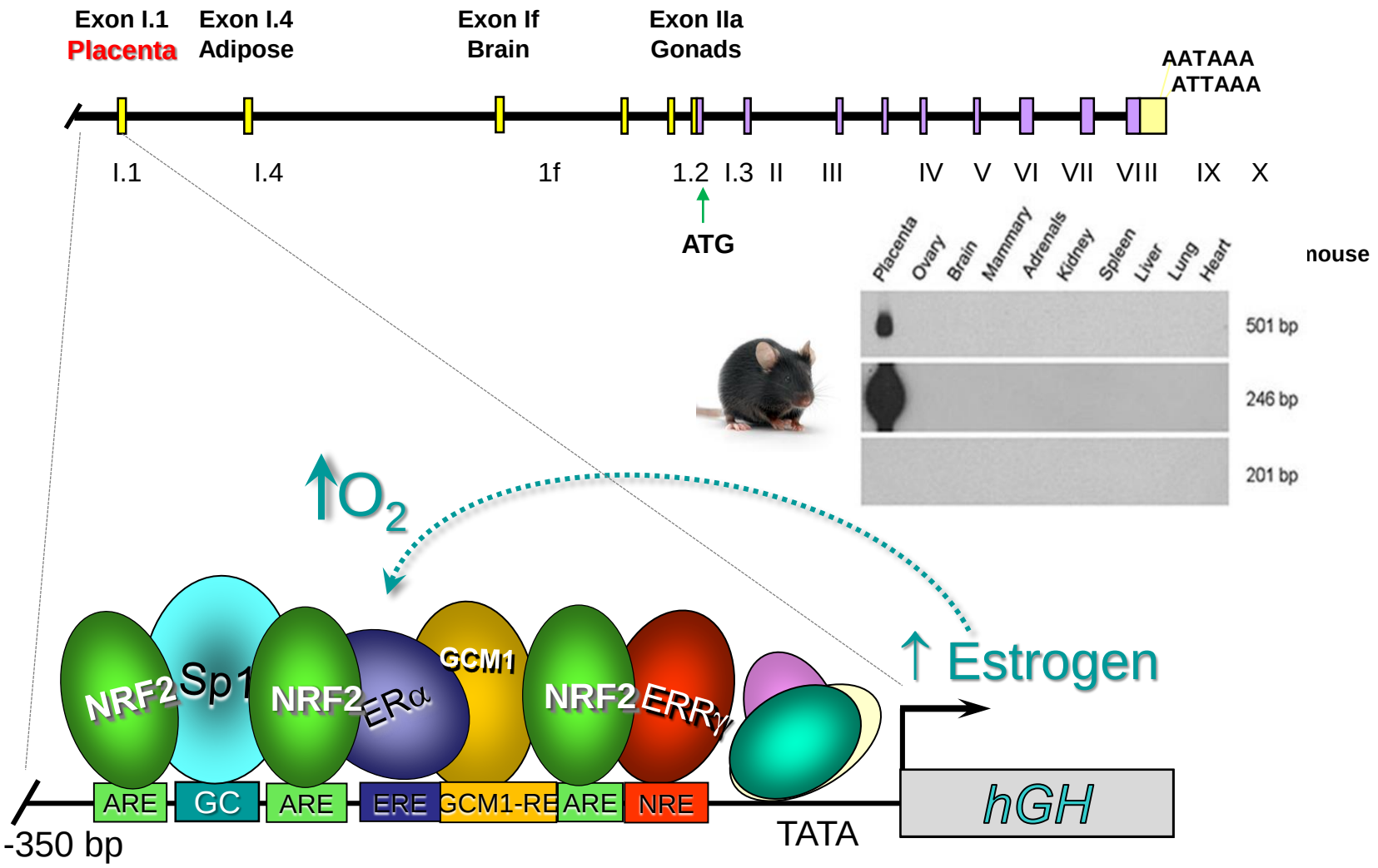
Exon I.1
Placenta
Exon I.4
Adipose
Exon If
Brain
Exon IIa
Gonads
AATAAA
ATTAAA
I.1
I.4
1f
1.2
I.3
II
III
IV
V
VI
VII
VIII
IX
X
ATG
Placenta
Ovary
Brain
Mammary
Adrenals
Kidney
Spleen
Liver
Lung
Heart
nouse
501 bp
246 bp
201 bp
↑O2
↑ Estrogen
NRF2
Sp1
NRF2
ERα
GCM1
NRF2
ERRγ
ARE
GC
ARE
ERE
GCM1-RE
ARE
NRE
-350 bp
TATA
hGH

Figure 4. Placenta-specific expression of human aromatase and its control by promoters and enhancers. Reproduced with the permission of the authors. Original figure provided by Dr Carol Mendelson.

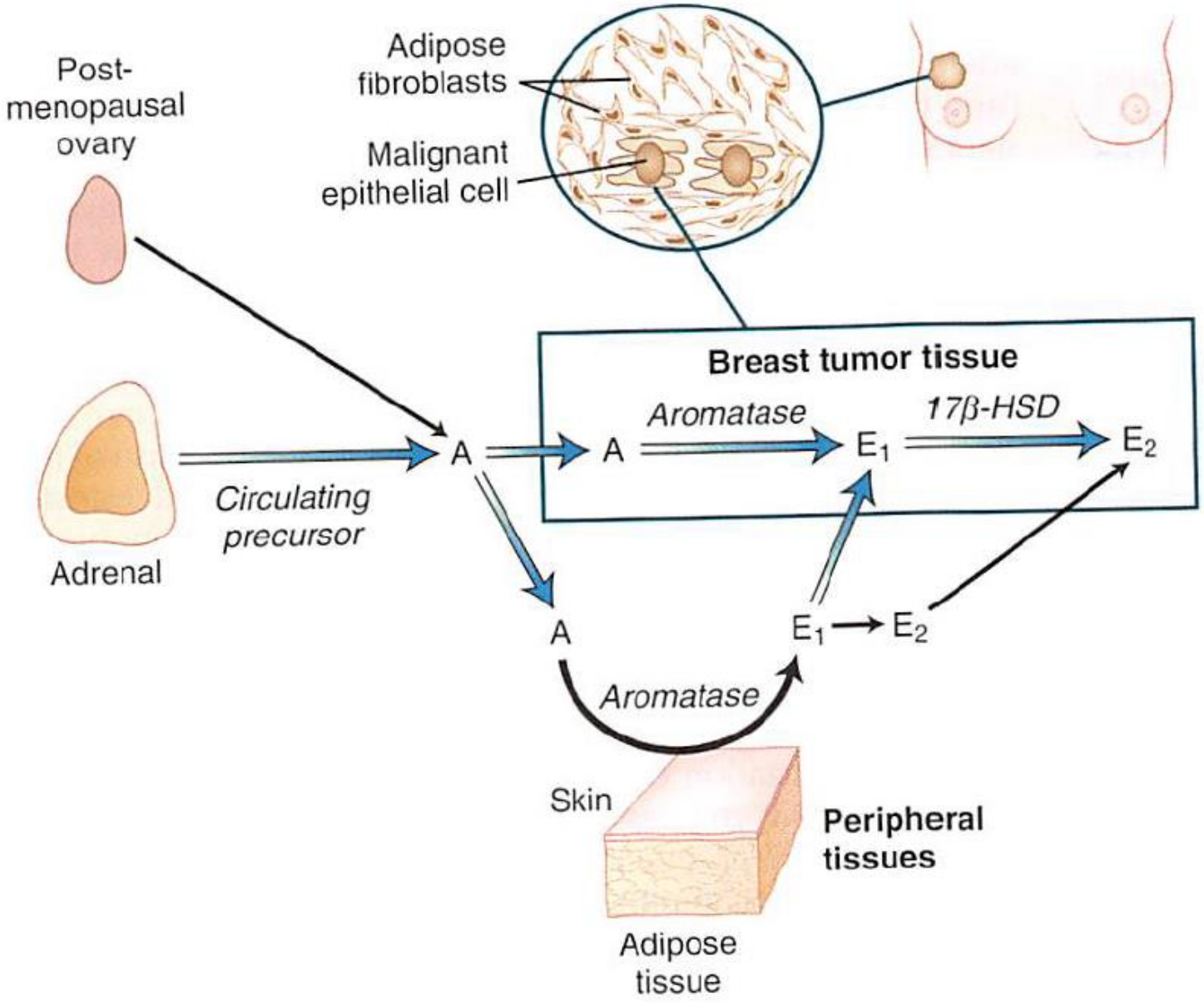
Post-
menopausal
ovary
Adipose
fibroblasts
Malignant
epithelial cell
Breast tumor tissue
Aromatase
17β-HSD
A
A
E1
E2
Circulating
precursor
Adrenal
A
E1
E2
Aromatase
Skin
Peripheral
tissues
Adipose
tissue

Figure 5. Concept of Intracrinology whereby steroids are synthesized in the tissue and act in that same tissue. In this figure, estradiol is synthesized in benign and malignant breast tissue via conversion of androstenedione to estrone (aromatase) and then to estradiol (17β-HSD). Reproduced from the chapter by Serdar E.Bulun in Williams Textbook of Endocrinology,13th Edition, chapter 17, Physiology and Pathology of the Female Reproductive System with the permission of the publishers for online and print versions.

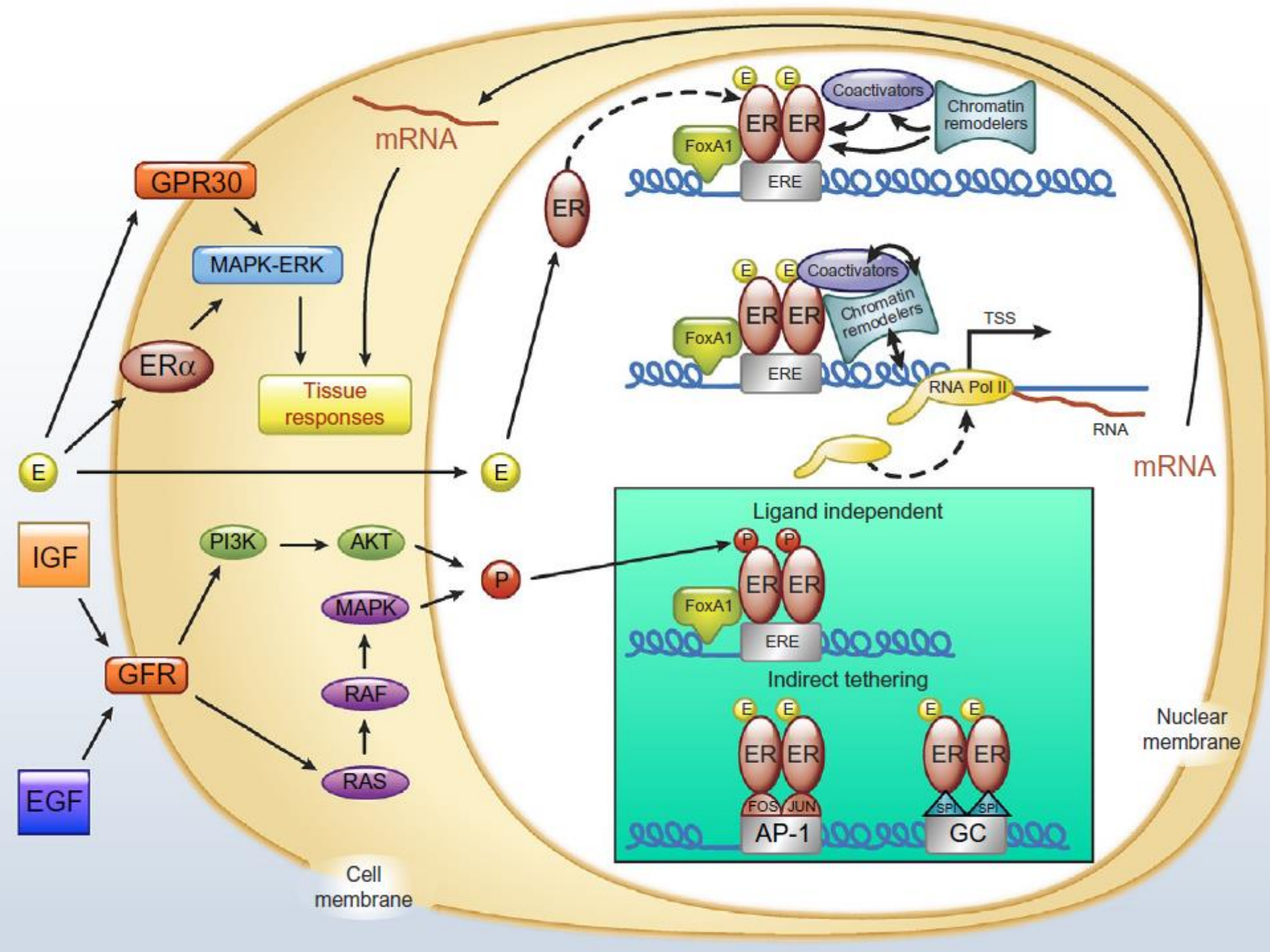
mRNA
GPR30
MAPK-ERK
ERα
Tissue responses
E
IGF
EGF
GFR
PI3K
AKT
MAPK
RAF
RAS
P
ER
E
E
ER ER
Coactivators
Chromatin remodelers
FoxA1
ERE
TSS
RNA Pol II
RNA
mRNA
Ligand independent
Indirect tethering
FOS
JUN
AP-1
SPI
SPI
GC
Nuclear membrane
Cell membrane

Figure 6. Diagram of the membrane-initiated and nuclear initiated effects of the estrogen receptor. Reproduced from (3) permission of the publishers for online and print versions.

Agonists and Antagonists Stabilize Distinct Conformations of the ER LBD
SERMs prevent the formation of an Active AF-2

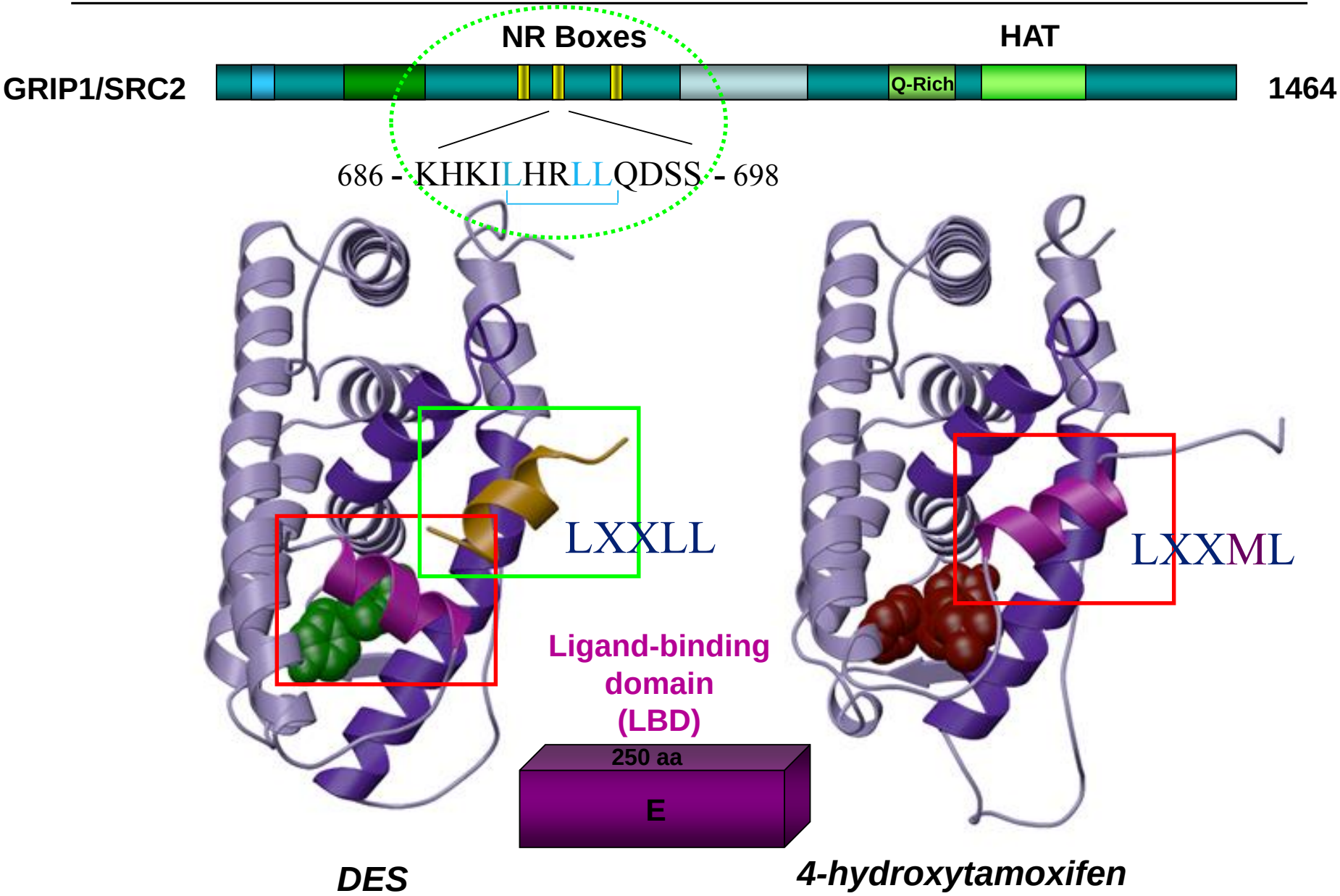

Shiau, et al., Cell (1998)

Figure 7. Crystal structure of the ER ligand binding domain (LBD) to which either DES (diethylstilbestrol) or 4-hydroxytamoxifen is bound. Original figure provided by Dr. Geof Greene which is adapted from (4) and with the permission of the publishers for online and print versions of this adaptation.

Metabolic and liver function parameters of man with aromatase deficiency

	before E treatment	after E treatment
metabolic parameters:		
• Total cholesterol (mg/dl)	177	110
• LDL cholesterol	107	66
• HDL cholesterol	31	41
• Triglycerides	199	106
• Glucose (70-110mg/dl)	180	144
• Insulin (5-30μU/ml)	94	53
• Fructosamine (μmol/L)	406	315
liver function parameters:		
• GPT (<37U/L)	195	70
• GOT (<40U/L)	108	45
• γ-GT (<11-50U/L)	153	42

Conclusions: estrogen regulates lipids, enhances insulin sensitivity, lowers glucose, normalizes liver function :

Figure 8. Metabolic and liver function parameters in a single male patient with aromatase deficiency. Reproduced with the permission of the publishlishers for the online and print versions (5).

Estrogen replacement reverses hepatic steatosis in male ArKO mice and in a man with aromatase deficiency

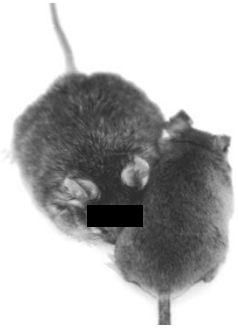

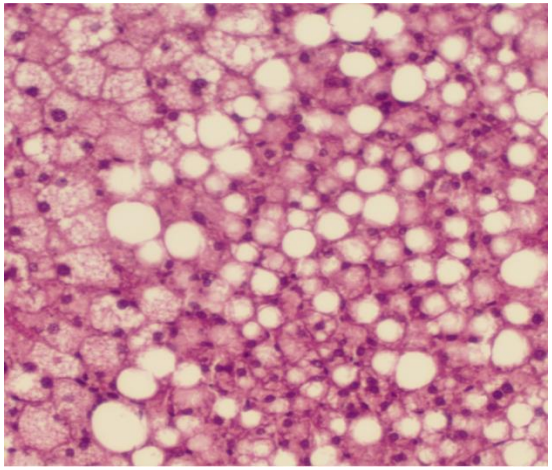

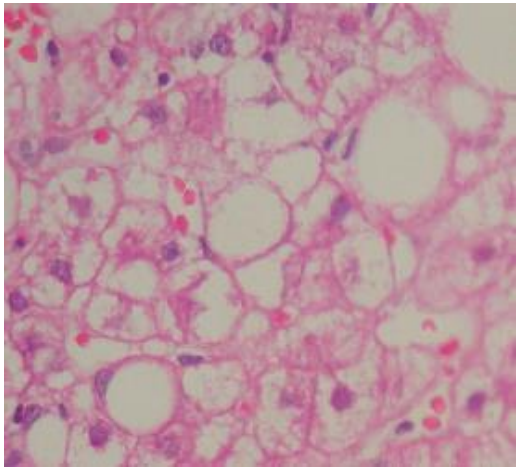

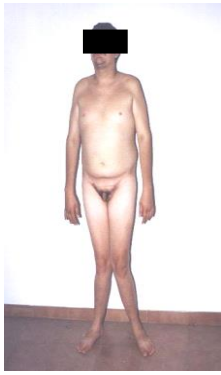

Before treatment

Before treatment

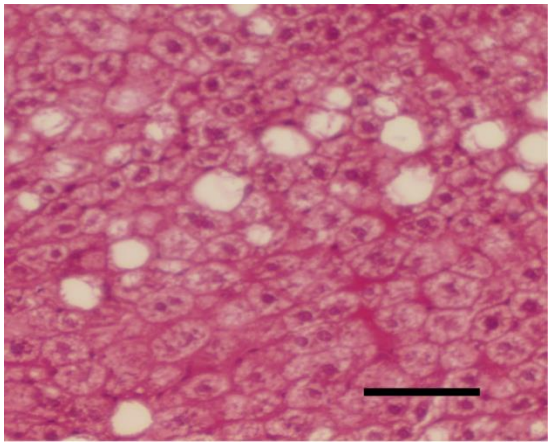

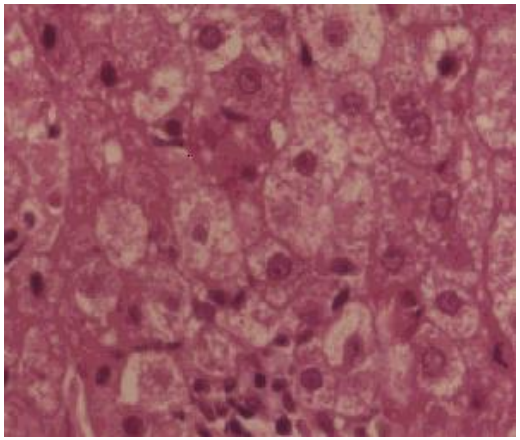

6 wks estradiol treatment

1 yr estradiol treatment

Hewitt 2004

Maffei et al. 2004

Figure 9.Illustration of the liver in an aromatase deficient mouse and in an aromatase deficient patient. From the studies of Hewitt and Simpson (6) and Maffei et al. Reproduced with the permission of the publishers for the online and print versions (5;7)

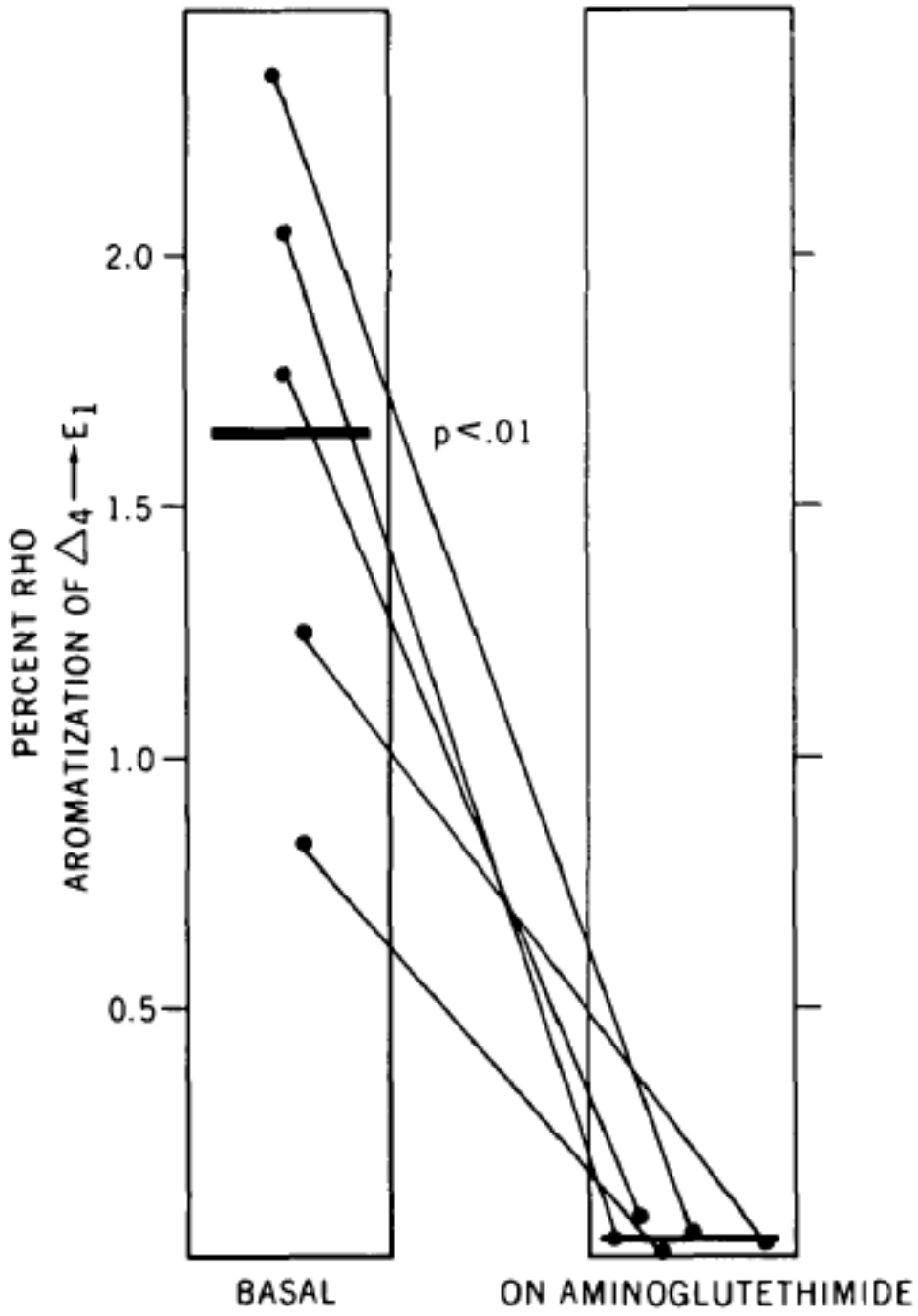
PERCENT RHO
AROMATIZATION OF $\Delta_4 \rightarrow E_1$
2.0
1.5
1.0
0.5
p<.01
BASAL
ON AMINOGLUTETHIMIDE

Figure 10. Effect of aminoglutethimide on whole body aromatase in post-menopausal women with breast cancer as demonstrated using the isotopic kinetic method for determining the percent conversion of androstenedione to estrone under steady state conditions (rho value) (8). Reproduced with the permission of the publisher for the online and print versions


4-OHA

Figure 11. The late Angela Brodie who developed the first steroidal aromatase inhibitor, 4-OH-androstenedione, to be tested in patients with breast cancer. Shown is a very large batch of 4-OH- androstenedione that was to be shipped to the United Kingdom for use in patients. Reproduced with the permission of her husband, Dr. Harry Brodie.

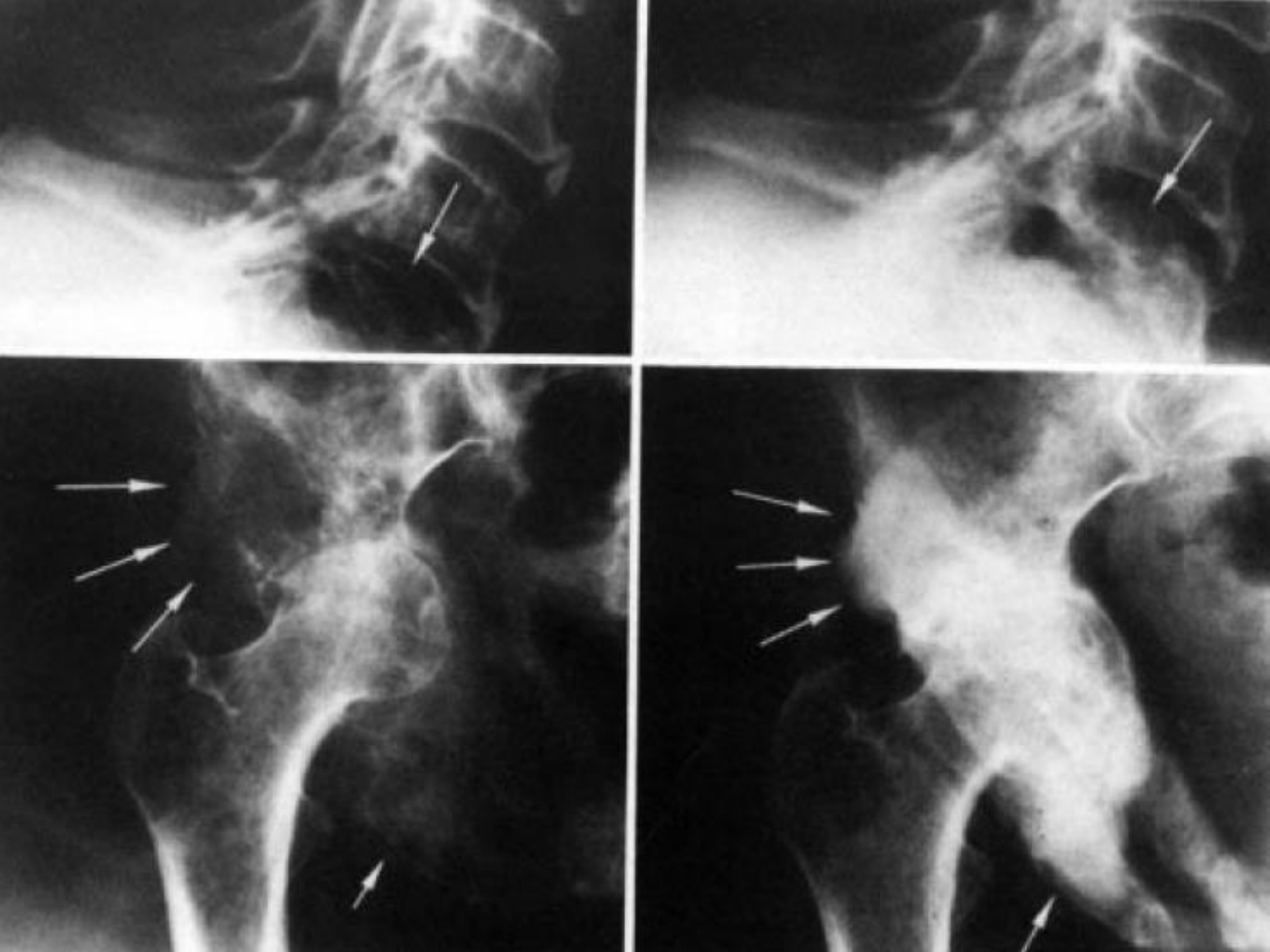

Figure 12. Effect of the aromatase inhibitor, aminoglutethimide, on the lytic bone metastases in a post-menopausal woman with breast cancer. Shown on the left are lytic lesions in the 7^{th} cervical vertebra (top panel) and the pelvis (bottom panel). Shown on the right panel are the comparable radiographs showing recalcification of the lytic lesions in response to suppression of estrogens production(9).Reproduced with the permission of the publishers for the online and print versions.

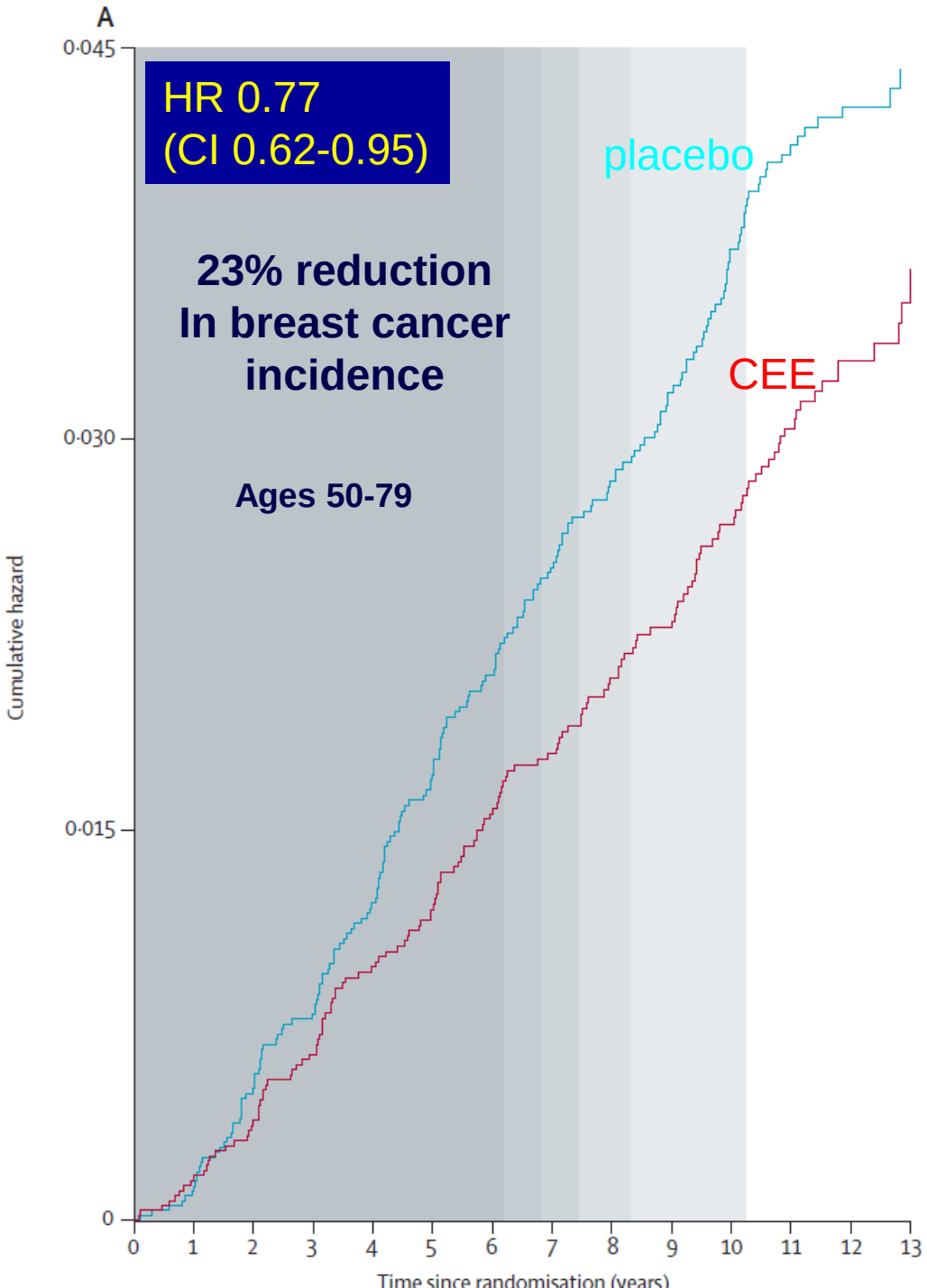
A
HR 0.77
(CI 0.62-0.95)
placebo
CEE
23% reduction
In breast cancer
incidence
Ages 50-79
Cumulative hazard
0·045
0·030
0·015
0
0
1
2
3
4
5
6
7
8
9
10
11
12
13
Time since randomisation (years)

Figure 13 . The thirteen year follow-up of women in the WHI (Women's Health Initiative) study who were treated with either placebo or CEE (conjugated equine estrogen). Reproduced with the permission of the publishers for the online and print versions. (10).